Published in final edited form as:

Eur Respir J. 2019 July ; 54(1): . doi:10.1183/13993003.02262-2018.

Quantifying the Magnitude of Pharyngeal Obstruction During Sleep Using Airflow Shape

Dwayne L Mann[*,1,2], **Philip I Terrill**[1,2], **Ali Azarbarzin**[2], **Sara Mariani**[2], **Angelo Franciosini**[3], **Alessandra Camassa**[4], **Thomas Georgeson**[1], **Melania Marques**[2,5], **Luigi Taranto-Montemurro**[2], **Ludovico Messineo**[2], **Susan Redline**[2], **Andrew Wellman**[2], **Scott A Sands**[2]

[1]School of Information Technology and Electrical Engineering, The University of Queensland, Brisbane, Australia.

[2]Division of Sleep and Circadian Disorders, Department of Medicine, Brigham & Women's Hospital & Harvard Medical School, Boston, MA, USA.

[3]Aix-Marseille Université, Marseille, France.

[4]Institut d'Investigacions Biomèdiques August Pi Sunyer (IDIBAPS), Barcelona, Spain.

[5]Laboratorio do Sono, Instituto do Coracao (InCor), Hospital das Clinicas, HCFMUSP, Faculdade de Medicina, Universidade de Sao Paulo, SP, BR.

Abstract

Rationale: Non-invasive quantification of the severity of pharyngeal airflow obstruction would enable recognition of obstructive versus central manifestation of sleep apnoea, and identification of symptomatic individuals with severe airflow obstruction despite a low apnoea-hypopnoea index (AHI).

Objectives: Here we provide a novel method that uses simple airflow-versus-time ("shape") features from individual breaths on an overnight sleep study to automatically and non-invasively quantify the *severity* of airflow obstruction without oesophageal catheterisation.

Methods: 41 individuals with suspected/diagnosed obstructive sleep apnoea (AHI range=0–91 events/hr) underwent overnight polysomnography with gold-standard measures of airflow (oronasal pneumotach, *flow*) and ventilatory drive (calibrated intraoesophageal diaphragm EMG, *drive*). Obstruction severity was defined as a continuous variable (*flow:drive* ratio). Multivariable regression used airflow shape features (inspiratory/expiratory timing, flatness, scooping, fluttering) to estimate *flow:drive* in 136,264 breaths (performance based on leave-one-patient-out cross-validation). Analysis was repeated using simultaneous nasal pressure recordings in a subset (N=17).

[*]Corresponding author: Dwayne Mann, School of Information Technology and Electrical Engineering, The University of Queensland, Brisbane, Australia, Tel: +61 407 134 208 Fax: +61 7 3365 4999, d.mann@uq.edu.au.

Author contributions: Study design: DM, PT, SS; Algorithm development: DM, AA, SM, AF, AC, SS. Data analysis: DM, PT, SS; Interpretation of results and Preparation of the Manuscript: All authors.

Measurement and Main Results: Gold-standard obstruction severity (*flow:drive*) varied widely across individuals independent of AHI. A multivariable model (25 features) estimated obstruction severity breath-by-breath (R^2=0.58 vs. gold-standard, P<0.00001; mean absolute error=22%) and the median obstruction severity across individual patients (R^2=0.69, P<0.00001; error=10%). Similar performance was achieved using nasal-pressure.

Conclusions: The severity of pharyngeal obstruction can be quantified non-invasively using readily-available airflow shape information. Our work overcomes a major hurdle necessary for the recognizing and phenotyping of patients with obstructive sleep disordered breathing.

Plain Language Summary

Pharyngeal airflow obstruction is a hallmark of obstructive sleep disordered breathing and manifests not only as changes in flow amplitude but also as changes in flow “shape” (flattening, scooping, timing, fluttering). There is currently no automated approach for using rich flow shape data to quantify the magnitude or severity of airflow obstruction during sleep. This information could improve sleep apnoea classification and phenotyping (e.g. central vs. obstructive pathophysiology) or airflow obstruction in the absence of cyclic respiratory events. First we introduce an objective definition of the severity of airflow obstruction, defined as the ratio of actual airflow to intended airflow or ventilatory drive (calibrated intraoesophageal diaphragm EMG, *drive*), where a *flow*:*drive* ratio of 50% indicates that the airflow achieved was half of the intended value (100% is an open airway; 0% is fully closed). We show that pharyngeal airflow obstruction varies widely for any given OSA severity (apnoea-hypopnoea index). Second we demonstrate that a multivariable model using automated flow shape information accurately estimates the severity of airflow obstruction: a) per breath (error=22%), and b) per patient (error=10%). Our approach overcomes major barriers for the objective phenotyping of sleep disordered breathing.

Keywords

Sleep apnoea; flow limitation; upper airway resistance; phenotyping

INTRODUCTION

Pharyngeal airflow obstruction, characterised by a mismatch between actual ventilatory *flow* and ventilatory effort (*drive)*, is a hallmark of obstructive sleep disordered breathing [1]. For decades, investigators have sought to assess airflow obstruction and consequent flow-limitation [2–4] for the purposes of phenotyping obstructive versus central contributions to sleep apnoea [5, 6], and for identifying individuals with a low apnoea-hypopnoea index (AHI) who have severe airflow obstruction and symptoms that may warrant treatment [7, 8]. It is now widely appreciated that the AHI is not a reliable indicator of sleep disordered breathing symptoms or outcomes, with several studies suggesting that the severity of airflow obstruction may be influential [9–15]. A non-invasive means to estimate of the severity of pharyngeal obstruction is needed [16].

The field of sleep medicine is now reinvigorating efforts to automatically detect pharyngeal obstruction (i.e. inspiratory flow limitation) based on the flow “shape” of individual breaths

[17, 18]. Clinically, pharyngeal obstruction is recognised by expert scientists based on: a flattening or scooping (mid-inspiratory dip) of inspiratory flow [19–21], an increase in inspiratory time at the expense of expiratory time [22], and complex flow-limited breath patterns involving intermittent collapse and fluttering [23]. Thus, it is feasible that these features could be combined to estimate the severity of airflow obstruction automatically.

Important progress has already been made: Automated methods to detect flow shape features currently form the underlying algorithms within auto-titrating CPAP machines [20], yet these algorithms are not publicly available [24]. The main limitation to the available published approaches [6, 18, 20, 25–28] has been the reliance on patient characteristics or subjective expert interpretation to classify presence or absence of obstruction, and most studies have limited methods to a single flow “shape” feature [6, 20].

Here we developed and validated a tool that combines flow shape features across multiple known domains (flattening, scooping, timing, fluttering) to estimate airflow obstruction objectively across a continuum of severities. First, we define airflow obstruction based on the ratio of actual ventilation (*flow*) to the intended ventilation based on calibrated intraoesophageal diaphragm EMG (*drive*), i.e. the *flow:drive* ratio [29, 30]. Second, flow shape features were calculated in participants with suspected or diagnosed obstructive sleep apnoea (N=41). A host of flow shape features (see Methods) were used to develop a multivariable model to estimate the severity of pharyngeal airflow obstruction (*flow:drive*) in individual breaths, and average obstruction severity in individual patients. Finally, we examined the performance of the same multivariable flow shapes model using the nasal pressure signal as a clinically-applicable means to quantify obstruction (N=17).

METHODS

Subjects

Forty-three participants with suspected or diagnosed obstructive sleep apnoea (OSA) attended our sleep research laboratory. All individuals with suspected but not diagnosed OSA reported witnessed snoring/gasping plus daytime sleepiness/fatigue. Patients were free of major co-morbidities and were not using medications expected to influence ventilatory control. The study was approved by the Partners Internal Review Board. All participants provided written informed consent before participation. Two participants could not tolerate oesophageal catheterisation (see below), leaving 41 patients with data available for analysis.

Procedure

In addition to routine polysomnographic signals (electroenchephalography, electrocardiography, thoracoabdominal movements, oximetry), airflow was measured with a pneumotach (Hans Rudolf, Shawnee KS, USA; Validyne Engineering, Northbridge CA, USA) attached to an oronasal mask (AirFit small, Resmed Inc., San Diego CA, USA). To provide gold-standard measurement of ventilatory drive, minimally influenced by changes in airflow [31], each patient was instrumented with an intraoesophageal diaphragmatic EMG catheter (Servo-i Ventilator, Maquet Getinge Group, Wayne, NJ, USA). A subset of patients

(N=17) had simultaneous nasal pressure recording via a modified cannula. Patients slept supine throughout the studies.

The physiological link between airflow obstruction and flow shape

Theory.—In principle, the flow "shape" (airflow versus time profile), manifest via pharyngeal obstruction, depends not only on the degree of collapsibility but also on the underlying ventilatory drive (Figure S1), and thus reflects the ratio of actual airflow (ventilation, referred to as *flow*) to intended ventilation (ventilatory drive, referred to as *drive*). Thus, this ratio "*flow*:*drive*" was used as a continuous quantitative measure of the severity of airflow obstruction, scaled so that 100% indicates a patent airway based on wakefulness [5, 29]; note *flow*:*drive*=50% indicates obstruction with actual flow equal to just half of the intended flow (*drive*) consequent to reduced flow and/or increased drive. The *flow*:*drive* definition of obstruction is intentionally broad to encompass any form of manifest flow-limitation (e.g. Starling resistor 'flatness', negative effort dependence 'scoopiness'), more complex airway obstruction (e.g. intermittent collapse), and simple linear increases in resistance, all encapsulated by their common effect to reduce ventilation for any given level of ventilatory drive (lowered *flow:drive*). In principle, *flow*:*drive* is equal to the reciprocal of the respiratory system neuro-mechanical *impedance* (linear equivalent, resistance and elastance, presented as a fraction of the average wakefulness levels).

Data analysis

Gold-standard measurement of airflow obstruction (flow:drive).—Periods with absent signals, artefact or non-zero CPAP were manually excluded. Breaths scored as obstructive apnoea were automatically excluded from flow-shape processing. All other breaths were analysed, regardless of sleep stage (wake, sleep, arousal). Breath-to-breath ventilation was measured using tidal volume × respiratory rate (L/min). Ventilatory drive was calculated using the processed diaphragm EMG excursions, calibrated to L/min using wakefulness data. See Supplement for details. *Flow:drive* was calculated as ventilation (L/min) divided by ventilatory drive (L/min) and expressed as a percentage.

Flow shape measures.—To provide a method with broad clinical utility we down-sampled airflow data (pneumotach and nasal pressure) to 25Hz, i.e. AASM *minimum* sampling rate [32]. Nasal pressure signals were linearised as appropriate [30] (Figure S2).

We included published features [6, 19, 20] in addition to novel metrics as candidates. For inclusion, features had to be independent of flow amplitude and able to be calculated without external information (e.g. reference breaths). In total, 85 candidate features were calculated for each breath to reflect aspects of flattening, scooping, asymmetry, breath timing, and high-frequency variability (spectral power). See Supplement for details (Table S1). Key features are highlighted in Results.

Features that were not well-characterised using nasal pressure ($R^2 \leq 0.5$ vs. pneumotach flow measures, ~40% of features, Table S2) were excluded since clinical application (nasal pressure) is a major goal of this work.

Flow-Shape Estimation of Obstruction Severity

We adopted a simplified "machine-learning" approach for face-validity and translatability:

Feature transformation.—To handle non-linear associations between flow shape features and obstruction severity, we made transformed versions of each feature (square and square-root) and untransformed versions all available for selection.

Multivariable regression to quantify airflow obstruction.—Multivariable linear regression with backwards elimination was employed to identify a model (set of feature terms and coefficients) for predicting obstruction severity (*flow:drive,* continuous variable).

Analysis of nasal pressure.—Flow shape features were assessed in 17 patients; the above model was used to estimate obstruction severity compared with the gold standard (*flow:drive* from pneumotach and diaphragm EMG).

Statistical Analysis

Reported estimates of *flow:drive* throughout the study were based on a conservative leave-one-patient-out cross-validation procedure, whereby *flow:drive* estimates from each patient were based on a modified version of the model using only other patients' data. The coefficient of determination (R^2) was used to assess the strength of the relationship between the gold standard obstruction severity (*flow:drive*) and the flow-shape-estimated for each breath (all data wake and sleep). The same approach was used to assess the association between the median obstruction severity (gold standard vs. estimated) for each patient (all breaths during sleep only, data in arousals excluded to assess sleep-related obstruction). $R^2>0.5$ was considered a strong association. Mean absolute error was used to describe the expected estimation error. Weighted least-squares was used in regression model development to balance the influence of five severity classes (normal: *flow:drive* >90%, mild: 70–90%, moderate: 50–70%, severe: 30–50%, very severe: <30%). $P<0.05$ was considered statistically significant. Multivariable regression assessed whether obstruction severity estimated from flow shape predicted the gold-standard (*flow:drive*) independent of obstruction frequency (AHI).

RESULTS

Participant characteristics are summarised in Table 1. In total, 136,264 breaths in 41 participants were assessed.

Relationship between airflow obstruction severity and OSA severity

Although we observed an association between median gold-standard obstruction severity (*flow:drive*) and OSA severity (apnoea-hypopnoea index), the median obstruction severity varied widely for any given obstruction frequency (AHI, residual SD = 23%; Figure 1). Some individuals had profound obstruction despite a low AHI.

Multivariable flow-shape estimate of airflow obstruction

Number of shape features.—Mean absolute error (estimated minus gold-standard, cross-validated) decreased with increasing numbers of shape features (beyond 100 features); a model with 25 features represented a sensible compromise between accuracy and complexity (Figure S3 and S4).

Examples.—Representative traces illustrate concordance between estimated and gold-standard obstruction severity (*flow:drive*) values in common clinical circumstances (Figure 2). Note how knowledge of obstruction provides quantifiable insight into the (otherwise covert) pathophysiology in each example.

Breath-by-breath obstruction.—The estimated obstruction severity for each breath (i.e. continuous *flow:drive* values predicted from flow shape model; pneumotach signal) was strongly associated with the gold standard *flow:drive* values (without cross-validation, R^2=0.63, mean absolute error = 18%; Figure 3A shows cross-validated results, R^2=0.58, P<0.00001, mean absolute error = 22%).

Patient average obstruction.—The estimated median obstruction severity for each patient during sleep were also strongly associated with gold-standard *flow:drive* values (without cross-validation, R^2=0.77, mean absolute error = 9%; Figure 3B shows cross-validated results, R^2=0.69, P<0.00001, mean absolute error = 10%). Adjusting for AHI did not diminish the association (P<0.00001).

Key flow-shape measures

The top 5 features captured high frequency variability (spectral power) in inspiration and expiration, deviation from a normal rounded contour in inspiration and expiration, and the degree of inspiratory scooping (Table 2, Figure 4). The complete list of 25 shape features utilized in the final model are described in Table S3.

Nasal pressure analysis

In total, 62,990 breaths with simultaneous nasal pressure (clinical airflow signal) and pneumotach oronasal airflow were assessed. Nasal pressure estimates of *flow:drive* (same model) were strongly associated with pneumotach derived estimates (R^2=0.80, P<0.00001, mean absolute error = 8%; Figure 5A, Table S3).

Using nasal pressure, the estimated obstruction severity for each breath (R^2=0.48, P<0.00001, mean absolute error = 23%; Figure 5B) and for each patient (R^2=0.46, P<0.00001, mean absolute error = 11%, adjusted for AHI: P=0.002; Figure 5C) were significantly associated with the gold standard *flow:drive.* Note that mean absolute errors were similar to the pneumotach estimates (i.e. 22%, 10% respectively).

DISCUSSION

The current study has developed and validated the first automated method for quantifying the *magnitude* of pharyngeal airflow obstruction during sleep using airflow shape on a

breath-by-breath basis. We provide a simple multi-feature model that estimates the breath-by-breath obstruction severity and provides an accurate estimate of average obstruction severity (which we show is considerably different from obstruction frequency, i.e. AHI). Use of nasal pressure was similarly effective illustrating that the current approach can be readily applied to a routine clinical sleep study. Overall, our study demonstrates that the flow shape can be leveraged to quantify the degree of pharyngeal obstruction during sleep, information which is not otherwise evident when assessing sleep apnoea severity.

Novel Physiological Insights

Our study demonstrates that magnitude of pharyngeal airflow obstruction (flow limitation) —measured *on a continuum* (ratio of ventilation to ventilatory drive, *flow:drive,* [30, 33]) —influences the clinically-observed flow shape in obstructive sleep disordered breathing. First, we showed that theoretically (Figure S1) the airflow shape generated by a flow-limited airway is fundamentally affected by both the properties of the airway (collapsibility, tube law, peak flow) as well as the ventilatory drive or effort, and that the ratio of these aspects (*flow:drive*) theoretically determines the observed flow shape. Second, by direct measurement in patients we demonstrated that a greater mismatch between flow and drive (airflow obstruction severity) is associated with multiple recognisable flow shape abnormalities (see Table S3), including greater signal variability (spectral power) in both inspiration and expiration [23], deviation from a rounded (“sinusoidal”) inspiratory flow contour [18], greater “scooping” [21], increased inspiratory time [6] and greater inspiratory flattening [20]. A brief summary of the highest performing features in the final model are presented in Table 2 and illustrated in Figure 4. Third, when combined, flow shape features can explain ~58% of the variability in *flow:drive*. Fourth, further analysis revealed that the flow shape associations with *flow* and *drive* assessed separately is somewhat weaker (R^2=0.45, 0.30 respectively, compared with 0.58 for *flow:drive* ratio) demonstrating that it is the mismatch between flow and drive (*flow:drive*) that best explains the manifest flow shape abnormalities in obstructive sleep disordered breathing.

Our study is the first to demonstrate that combined airflow shape features can be used as a tool to recognise the otherwise concealed severity of airflow obstruction on a breath-by-breath basis. Bivariate analysis showed that there was no single shape feature with high predictive performance across the patient cohort (Table S1). For example, increased inspiratory duty ratio (inspiratory duration ÷ total breath duration) [28] was modestly associated with obstruction severity (R^2=0.32), and a well-known inspiratory flattening index used for CPAP titration [20] also performed modestly (R^2=0.34). Combining multiple features was considerably more effective (R^2=0.58), consistent with the knowledge that pharyngeal obstruction manifests as different flow shapes in different patients [21, 23, 25].

Clinical Implications

A major goal of the field for decades has been a non-invasive clinically-applicable automated method to quantify the magnitude of airflow obstruction on individual breaths using a clinically-accessible airflow signal (nasal pressure) for the purposes of 1) detecting obstructive sleep disordered breathing (i.e. *upper airway resistance syndrome* [12, 34, 35])

in patients with minimal overt respiratory events and 2) facilitating discrimination between obstructive and central phenotypes of sleep apnoea.

It is well recognised that the symptoms of sleep-disordered breathing are not well explained by the frequency of respiratory events (AHI), and that there are a number of symptomatic individuals with severe unrecognised flow limitation (i.e. *upper airway resistance syndrome* [12, 34, 35]) who may benefit from treatment [9–15]. Available evidence has also demonstrated that hallmarks of greater obstruction severity—including increased oesophageal pressure swings, loud snoring—are associated with sleepiness and hypertension independent of the AHI [9–15]. For example, surgical treatment of flow limitation in a small study of children was effective at relieving symptoms [12], CPAP treatment of flow limitation in pregnancy can improve preeclampsia [14], and surgical treatment of flow limitation in adults may improve sleepiness [13]. However, the role of obstruction severity in the absence of overt apnoeas and hypopnoeas has remained poorly investigated due to the lack of objective and clinically-applicable measurement techniques. Indeed, a recent American Thoracic Society working group [17] emphasised the need to develop an automated open-source algorithm (full model is provided in Supplement), with clear recommendations for recording standards (minimum 25 Hz sampling, DC-coupled, unfiltered), capable of using flow shape to detect airflow obstruction of both non-episodic and episodic nature, that could be related to clinical outcomes in epidemiological studies. Our method addresses and exceeds these requirements by (a) identifying and utilising an objective physiological gold standard (rather than subjective expert-consensus-guided labels), and (b) quantifying the magnitude of pharyngeal obstruction on a continuum.

The differential diagnosis of central versus obstructive sleep apnoea is challenging due to difficulty determining the severity of obstruction during sleep. Importantly, treatments for sleep apnoea that target pharyngeal anatomy (CPAP, oral appliances, surgery) are consistently less efficacious in those with a more central (or high loop gain) phenotype [36–38]. By definition, this non-obstructive (possibly “central”) phenotype manifests as the presence of respiratory events despite minimal obstruction severity (e.g. Figure 1(ii)). An estimate such as the median obstruction severity during sleep, which had minimal error (10% pneumotach, 11% nasal pressure) and was not confounded by AHI, is needed if such patients are to be easily identified for future phenotype-based interventions.

We emphasise that our approach is clinically applicable by design and seeks to obviate the requirement for (invasive) oesophageal catheterisation. Further studies are needed to test the utility of the tool, and determine the role of the severity of airflow obstruction *per se* in the sequelae of sleep disordered breathing.

Methodological considerations

There are a number of methodological considerations. Our definition of *flow:drive* is calibrated based on wake respiratory mechanics, and as such, the calibration value may change across the night. To control for this, the calibration value was extrapolated using a weighted moving-time average to best represent changes across the night. The calibration to wakefulness also means that our gold standard measure of airflow obstruction is expressed relative to wakefulness (i.e. relative resistance) rather than absolute obstruction (i.e. absolute

resistance); thus deficits in wake mechanics will not be detected (e.g. underestimating absolute resistance in obese patients with wake deficits). We emphasise that our goal was to describe sleep-specific changes. Second, we chose a relatively simple feature selection and classification routine (multivariable linear regression with stepwise feature selection) to train and validate our model to ensure face validity and ease of sharing with other investigators. We performed a separate validation study (N=29, see Supplement for details) that showed that the current method had positive predictive value of 88% and negative predictive value of 85% to detect obstructed breaths (in hypopneas) versus unobstructed breaths (in arousals). It is possible that further performance improvements could be achieved by the use of more sophisticated classification tools, however such approaches can obfuscate important discriminatory features. Likewise, combining input from other physiological indicators of airflow obstruction (e.g. respiratory belts, oximetry, snoring sounds, transcutaneous CO_2) may improve model performance [39]. We also note that our method does not require an unusual signal quality: we intentionally used signals down-sampled to 25 Hz to represent a standard clinical polysomnogram (maximising clinical applicability). While increased signal quality might be expected to improve the method, a recent study found that lowering sampling rate to 25 Hz did not greatly affect ability to detect presence/absence of flow-limitation [40], provided the sampling rate was similar during development and testing.

The current study made no attempt to use flow shape to estimate the site of collapse or to estimate the timing of pharyngeal collapse with respect to the phases of the respiratory cycle. However, we have inherently taken into account—through the various candidate flow shapes that capture aspects of both inspiratory and expiratory skewness and asymmetry—the understanding that the timing of obstruction is heterogeneous.

Our measure of obstruction severity (*flow:drive*) does not, by itself capture the balance between central and obstructive contributions to loss of flow during hypopnoeas, or capture the absolute drop in drive per se. Recognition of a “central phenotype” may require not only specific consideration of *flow:drive* during events, but also assessment of flow, and the evolution of these measures across the course of events: We would consider hypopnoeas to be of 1) classic “obstructive” manifestation if drive rises while flow falls throughout a hypopnoea, recognizable by a fall in *flow:drive* that occurs faster in comparison to the fall in flow (i.e. drive increases), and 2) more “central” in manifestation (than classic obstruction) if flow falls in parallel with a fall in drive (with obstruction nonetheless present when flow falls faster than drive, e.g. Figure 2D), recognizable by a fall in *flow:drive* that occurs slower than the fall in flow (i.e. drive decreases). See Supplement, Figure S8, for examples. Future studies validating the utility of these approaches with respect to clinical outcomes of therapy are warranted.

Conclusions

We provide a method for the quantification of pharyngeal airflow obstruction that uses information derived entirely from the airflow shape of any given breath. The method compared favorably against a physiological gold standard, on a breath-by-breath basis and when assessing average patient obstruction during sleep. Use of nasal pressure did not yield a substantial deterioration in performance, indicating that our technique is ready

for application to routine clinical polysomnography. As such, our work provides tools needed to address the long-standing inability to discriminate between obstructive and non-obstructive manifestations of sleep apnoea, with implications for guiding sleep apnoea therapies. Likewise, it may enable recognition of a disturbing magnitude of pharyngeal airway obstruction in symptomatic non-apneic individuals who are presently ineligible for treatment of sleep disordered breathing on the basis of a low AHI.

Supplementary Material

Refer to Web version on PubMed Central for supplementary material.

Acknowledgments

Funding sources: This work was supported by a grant from the National Health and Medical Research Council of Australia (NHMRC; 1064163) and the National Institute of Health (NIH; R01HL128658). Mr Mann was supported by a University of Queensland Research Scholarship and Graduate School International Travel Award. Dr. Sands was supported by the American Heart Association (15SDG25890059), an NHMRC Early Career Fellowship and R.G. Menzies award (1053201), an American Thoracic Society Foundation Unrestricted Grant. Dr. Mariani was supported as a coinvestigator of NIH grants (R24HL114473, U01HL119991, and R35HL135818).

REFERENCES

1. Ayappa I, Rapoport DM. The upper airway in sleep: physiology of the pharynx. Sleep medicine reviews 2003: 7(1): 9–33. [PubMed: 12586528]
2. Calero G, Farre R, Ballester E, Hernandez L, Daniel N, Montserrat Canal JM. Physiological consequences of prolonged periods of flow limitation in patients with sleep apnea hypopnea syndrome. Respiratory medicine 2006: 100(5): 813–817. [PubMed: 16388943]
3. de Godoy LB, Palombini LO, Martinho Haddad FL, Rapoport DM, de Aguiar Vidigal T, Klichouvicz PC, Tufik S, Togeiro SM. New insights on the pathophysiology of inspiratory flow limitation during sleep. Lung 2015: 193(3): 387–392. [PubMed: 25827757]
4. Palombini LO, Tufik S, Rapoport DM, Ayappa IA, Guilleminault C, de Godoy LB, Castro LS, Bittencourt L. Inspiratory flow limitation in a normal population of adults in Sao Paulo, Brazil. Sleep 2013: 36(11): 1663–1668. [PubMed: 24179299]
5. Randerath WJ, Treml M, Priegnitz C, Stieglitz S, Hagmeyer L, Morgenstern C. Evaluation of a noninvasive algorithm for differentiation of obstructive and central hypopneas. Sleep 2013: 36(3): 363–368. [PubMed: 23450252]
6. Mooney AM, Abounasr KK, Rapoport DM, Ayappa I. Relative prolongation of inspiratory time predicts high versus low resistance categorization of hypopneas. Journal of clinical sleep medicine : JCSM : official publication of the American Academy of Sleep Medicine 2012: 8(2): 177–185. [PubMed: 22505863]
7. Guilleminault C, Stoohs R. Arousal, increased respiratory efforts, blood pressure and obstructive sleep apnoea. Journal of sleep research 1995: 4(S1): 117–124. [PubMed: 10607187]
8. Chandra S, Sica AL, Wang J, Lakticova V, Greenberg HE. Respiratory effort-related arousals contribute to sympathetic modulation of heart rate variability. Sleep & breathing = Schlaf & Atmung 2013: 17(4): 1193–1200. [PubMed: 23417318]
9. Nakano H, Hirayama K, Sadamitsu Y, Shin S, Iwanaga T. Mean tracheal sound energy during sleep is related to daytime blood pressure. Sleep 2013: 36(9): 1361–1367. [PubMed: 23997370]
10. Stoohs R, Guilleminault C. Snoring during NREM sleep: respiratory timing, esophageal pressure and EEG arousal. Respiration physiology 1991: 85(2): 151–167. [PubMed: 1947456]
11. Guilleminault C, Stoohs R, Shiomi T, Kushida C, Schnittger I. Upper airway resistance syndrome, nocturnal blood pressure monitoring, and borderline hypertension. Chest 1996: 109(4): 901–908. [PubMed: 8635368]

12. Guilleminault C, Winkle R, Korobkin R, Simmons B. Children and nocturnal snoring: evaluation of the effects of sleep related respiratory resistive load and daytime functioning. Eur J Pediatr 1982: 139(3): 165–171. [PubMed: 7160405]
13. Newman JP, Clerk AA, Moore M, Utley DS, Terris DJ. Recognition and surgical management of the upper airway resistance syndrome. The Laryngoscope 1996: 106(9 Pt 1): 1089–1093. [PubMed: 8822711]
14. Edwards N, Blyton DM, Kirjavainen T, Kesby GJ, Sullivan CE. Nasal continuous positive airway pressure reduces sleep-induced blood pressure increments in preeclampsia. American journal of respiratory and critical care medicine 2000: 162(1): 252–257. [PubMed: 10903250]
15. Pepin JL, Guillot M, Tamisier R, Levy P. The upper airway resistance syndrome. Respiration; international review of thoracic diseases 2012: 83(6): 559–566. [PubMed: 22377755]
16. Rapoport DM. On beyond Zebra (and the Apnea-Hypopnea Index) in Obstructive Sleep Apnea. American journal of respiratory and critical care medicine 2018: 197(9): 1104–1106. [PubMed: 29490151]
17. Pamidi S, Redline S, Rapoport D, Ayappa I, Palombini L, Farre R, Kirkness J, Pepin JL, Polo O, Wellman A, Kimoff RJ, American Thoracic Society Ad Hoc Committee on Inspiratory Flow L. An Official American Thoracic Society Workshop Report: Noninvasive Identification of Inspiratory Flow Limitation in Sleep Studies. Annals of the American Thoracic Society 2017: 14(7): 1076–1085. [PubMed: 28665698]
18. Zhi YX, Vena D, Popovic MR, Bradley TD, Yadollahi A. Detecting inspiratory flow limitation with temporal features of nasal airflow. Sleep Med 2018: 48: 70–78. [PubMed: 29860189]
19. Hosselet JJ, Norman RG, Ayappa I, Rapoport DM. Detection of flow limitation with a nasal cannula/pressure transducer system. American journal of respiratory and critical care medicine 1998: 157(5 Pt 1): 1461–1467. [PubMed: 9603124]
20. Teschler H, Berthon-Jones M, Thompson AB, Henkel A, Henry J, Konietzko N. Automated continuous positive airway pressure titration for obstructive sleep apnea syndrome. American journal of respiratory and critical care medicine 1996: 154(3 Pt 1): 734–740. [PubMed: 8810613]
21. Genta PR, Sands SA, Butler JP, Loring SH, Katz ES, Demko BG, Kezirian EJ, White DP, Wellman A. Airflow Shape Is Associated With the Pharyngeal Structure Causing OSA. Chest 2017: 152(3): 537–546. [PubMed: 28651794]
22. Onal E, Lopata M. Respiratory timing during NREM sleep in patients with occlusive sleep apnea. Journal of applied physiology 1986: 61(4): 1444–1448. [PubMed: 3781959]
23. Azarbarzin A, Marques M, Sands SA, Op de Beeck S, Genta PR, Taranto-Montemurro L, de Melo CM, Messineo L, Vanderveken OM, White DP, Wellman A. Predicting epiglottic collapse in patients with obstructive sleep apnoea. Eur Respir J 2017: 50(3).
24. Brown LK. Autotitrating CPAP: how shall we judge safety and efficacy of a “black box”? Chest 2006: 130(2): 312–314. [PubMed: 16899825]
25. Aittokallio T, Malminen JS, Pahikkala T, Polo O, Nevalainen OS. Inspiratory flow shape clustering: an automated method to monitor upper airway performance during sleep. Computer methods and programs in biomedicine 2007: 85(1): 8–18. [PubMed: 17084481]
26. Clark SA, Wilson CR, Satoh M, Pegelow D, Dempsey JA. Assessment of inspiratory flow limitation invasively and noninvasively during sleep. American journal of respiratory and critical care medicine 1998: 158(3): 713–722. [PubMed: 9730995]
27. Ayappa I, Norman RG, Krieger AC, Rosen A, O’Malley R L, Rapoport DM. Non-Invasive detection of respiratory effort-related arousals (REras) by a nasal cannula/pressure transducer system. Sleep 2000: 23(6): 763–771. [PubMed: 11007443]
28. Schneider H, Krishnan V, Pichard LE, Patil SP, Smith PL, Schwartz AR. Inspiratory duty cycle responses to flow limitation predict nocturnal hypoventilation. Eur Respir J 2009: 33(5): 1068–1076. [PubMed: 19129290]
29. Catcheside P, Reynolds K, Stadler D, McEvoy D. Ventilatory Effort Versus Output In Obstructive Sleep Apnoea Assessed Via The Respiratory System Equation Of Motion. In: Journal of sleep research; 2014; 2014. p. 59.
30. Sands SA, Edwards BA, Terrill PI, Taranto-Montemurro L, Azarbarzin A, Marques M, Hess LB, White DP, Wellman A. Phenotyping Pharyngeal Pathophysiology using Polysomnography in

Patients with Obstructive Sleep Apnea. American journal of respiratory and critical care medicine 2018: 197(9): 1187–1197. [PubMed: 29327943]

31. Luo YM, Wu HD, Tang J, Jolley C, Steier J, Moxham J, Zhong NS, Polkey MI. Neural respiratory drive during apnoeic events in obstructive sleep apnoea. Eur Respir J 2008: 31(3): 650–657. [PubMed: 18032443]
32. Iber C, Ancoli-Israel S, Chesson ALJ, Quan SF. The AASM manual for the scoring of sleep and associated events: rules, terminology and technical specifications. . 1 ed. American Academy of Sleep Medicine, Westchester, IL, 2007.
33. Catcheside PG, Reynolds K, Stadler D, McEvoy D. Ventilatory effort versus output in obstructive sleep apnea assessed by the respiratory system equation of motion [Abstract]. Sleep and Biological Rhythms 2014: 12 (Suppl. 1): 59.
34. Downey R 3rd, Perkin RM, MacQuarrie J. Upper airway resistance syndrome: sick, symptomatic but underrecognized. Sleep 1993: 16(7): 620–623. [PubMed: 8290854]
35. Douglas NJ. Upper Airway Resistance Syndrome Is Not a Distinct Syndrome. American journal of respiratory and critical care medicine 2000: 161(5): 1413–1415. [PubMed: 10806129]
36. Bradley TD, Logan AG, Kimoff RJ, Series F, Morrison D, Ferguson K, Belenkie I, Pfeifer M, Fleetham J, Hanly P, Smilovitch M, Tomlinson G, Floras JS, Investigators C. Continuous positive airway pressure for central sleep apnea and heart failure. The New England journal of medicine 2005: 353(19): 2025–2033. [PubMed: 16282177]
37. Edwards BA, Andara C, Landry S, Sands SA, Joosten SA, Owens RL, White DP, Hamilton GS, Wellman A. Upper-Airway Collapsibility and Loop Gain Predict the Response to Oral Appliance Therapy in Patients with Obstructive Sleep Apnea. American journal of respiratory and critical care medicine 2016: 194(11): 1413–1422. [PubMed: 27181367]
38. Joosten SA, Leong P, Landry SA, Sands SA, Terrill PI, Mann D, Turton A, Rangaswamy J, Andara C, Burgess G, Mansfield D, Hamilton GS, Edwards BA. Loop Gain Predicts the Response to Upper Airway Surgery in Patients With Obstructive Sleep Apnea. Sleep 2017: 40(7).
39. Kaplan V, Zhang JN, Russi EW, Bloch KE. Detection of inspiratory flow limitation during sleep by computer assisted respiratory inductive plethysmography. Eur Respir J 2000: 15(3): 570–578. [PubMed: 10759455]
40. Camassa A, Franciosini A, Sands SA, Zhi YX, Yadollahi A, Bianchi AM, Wellman A, Redline S, Azarbarzin A and Mariani S. Validating an algorithm for automatic scoring of Inspiratory Flow Limitation within a range of recording settings. In: 40th Annual International Conference of the IEEE Engineering in Medicine & Biology Society (EMBC); 2018; Honolulu, HI, USA; 2018.

Take-Home Message

The degree of pharyngeal airflow obstruction varies widely for any given OSA severity (apnoea-hypopnoea index) and is challenging to measure. Here we combine information from automated flow shape to accurately estimate the severity of airflow obstruction.

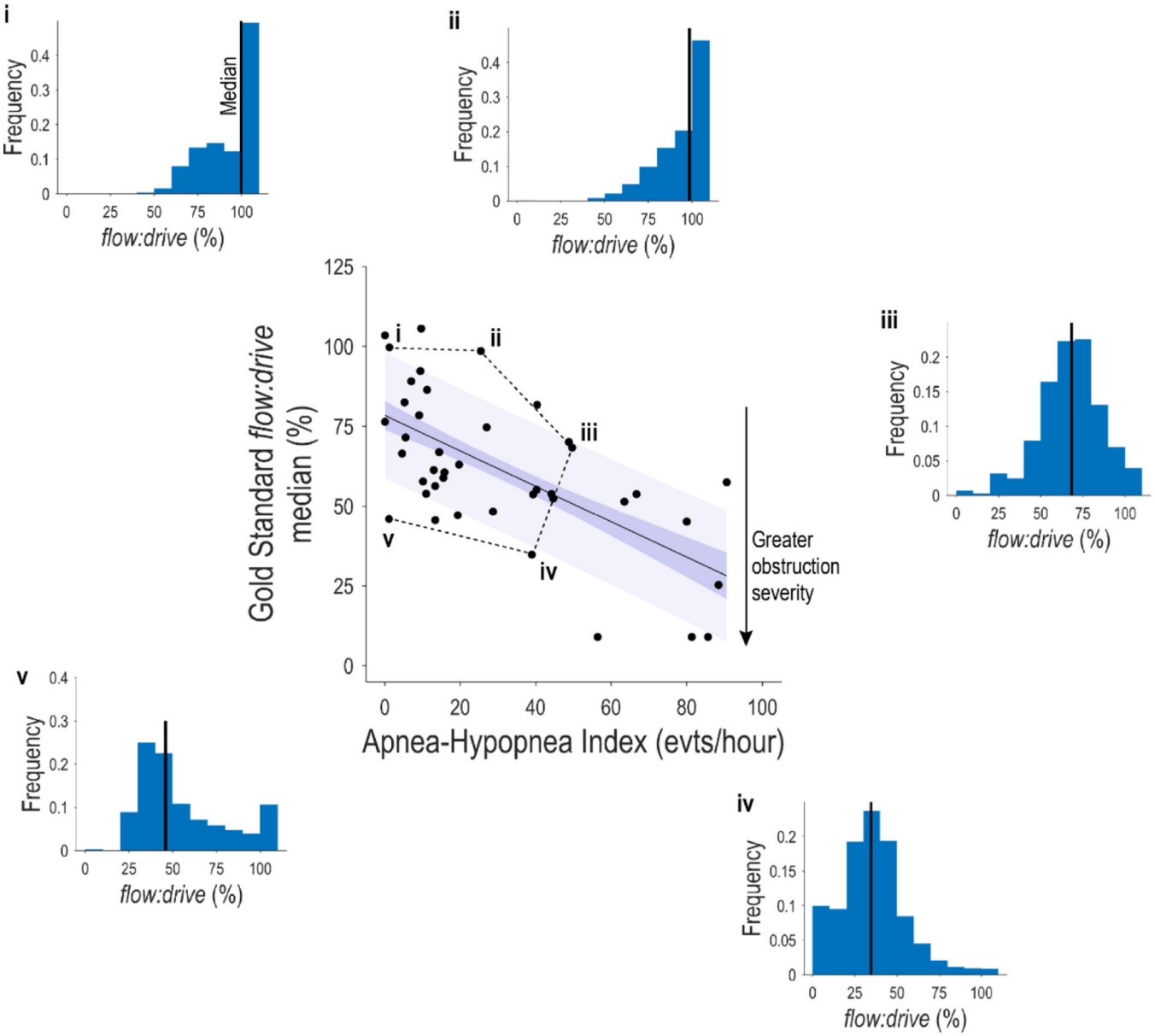

Figure 1:

Scatter plot (center) illustrates the association between the severity of airflow obstruction (gold-standard patient median *flow:drive*) and the frequency of airflow obstruction (apnoea-hypopnoea index) during sleep. Only the latter is currently reported clinically. Note some individuals without sleep apnoea (near zero AHI) exhibit substantial airflow obstruction (lowered median *flow:drive*). **Histograms** of airflow obstruction severity (*flow:drive)* during sleep for selected individuals (labelled i-v, matched with scatter plot): **(i)** Normal breathing: This individual neither has sleep apnoea nor airflow obstruction (median *flow:drive*=100%). **(ii)** Moderate sleep apnoea despite normal airflow obstruction (*flow:drive*=99%) suggesting a non-obstructive (possibly central) phenotype of sleep apnoea. **(iii)** Severe sleep apnoea without severe obstruction (*flow:drive*=65%), also suggesting a non-obstructive (possibly central) phenotype. **(iv)** Severe sleep apnoea with

severe airflow obstruction (*flow:drive*=35%). **(v)** No sleep apnoea despite a level of airflow obstruction (*flow:drive*=46%) consistent with severe OSA (e.g. iv).

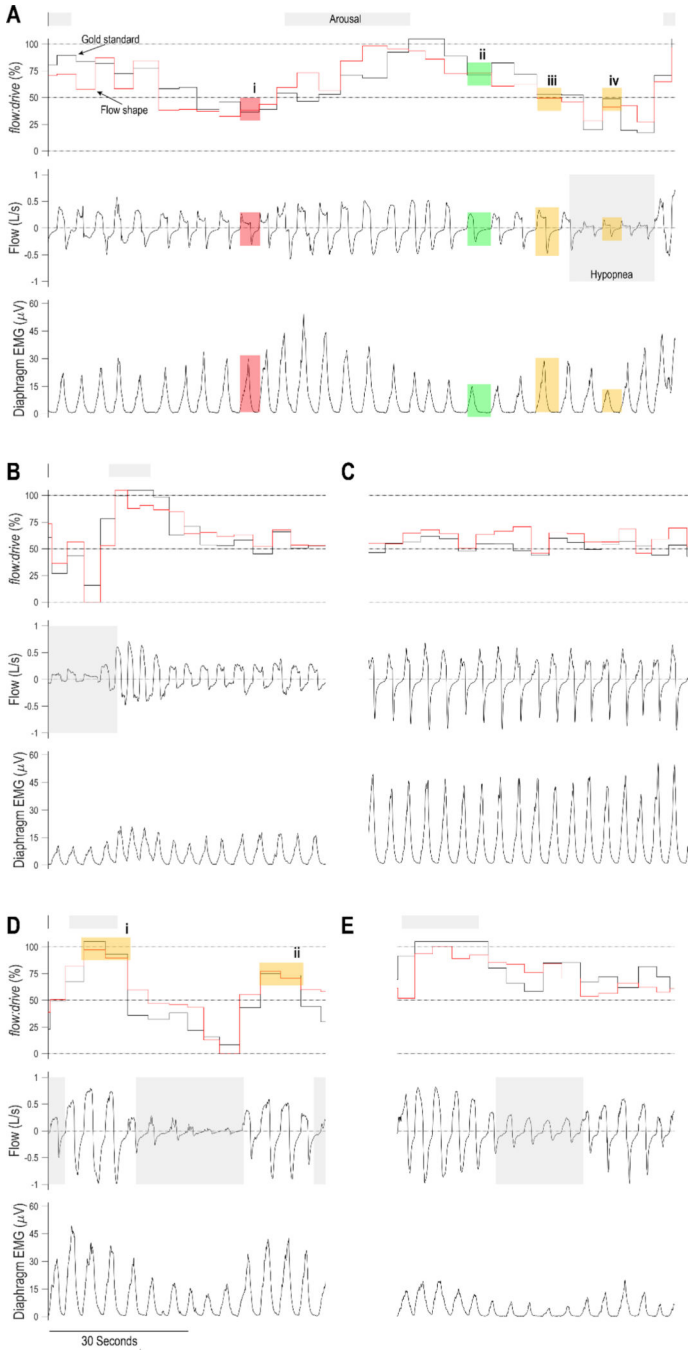

Figure 2:

Example patterns of airflow obstruction in five individuals (A-E). In each individual, note that the severity of airflow obstruction (*flow:drive*) estimated based on flow shape (red) matches the gold standard (black); flow and drive signals are shown separately. **(A)** First, note that in breath (**i**) the patient does not achieve the airflow that they intended based on drive (lowered *flow:drive*), which is evident based on the characteristic flow-limited "shape". Compare with breath (**ii**), where the same flow is achieved but at a lower drive; note the rounded "shape" when the airway is unobstructed. Second, note that breaths (**iii**)

and (**iv**) have different magnitudes but identical shapes, consistent with the parallel reduction in flow and drive in (**iv**) i.e. same obstruction severity. **(B)** Transition from cyclic events to "stable" breathing in a patient with sleep apnoea. Despite so called stable breathing, pharyngeal obstruction remains substantial (the patient achieves just half the intended flow, *flow:drive*=50%), a phenomenon that is recognisable based on flow shape. **(C)** Prolonged obstructed breathing without respiratory events, characterised by increased ventilatory drive, again recognisable based on flow shape. **(D)** At the end of one respiratory event, the airway is fully reopened in association with an arousal (**i**). A subsequent obstructive event is terminated without complete airway reopening (*flow:drive*<100%) in the absence of an arousal (**ii**), illustrating that this patient can achieve marked airflow recovery while maintaining sleep. In this interesting example, we also see the ventilatory drive is falling rather than rising during the event, while the airway is simultaneously becoming obstructed. We note that drive falls towards normal eupneic levels, while flow falls to ~10% of eupneic levels, i.e. the reduction in flow is proportionately greater than the reduction in drive, hence obstruction (reduced *flow:drive*). **(E)** A central hypopnoea, characterised by a reduction in flow that is similar in magnitude to the reduction in drive (diaphragm EMG), hence minimal obstruction (and high, constant *flow:drive*). In this case, the airway is more obstructed after (versus during) the event.

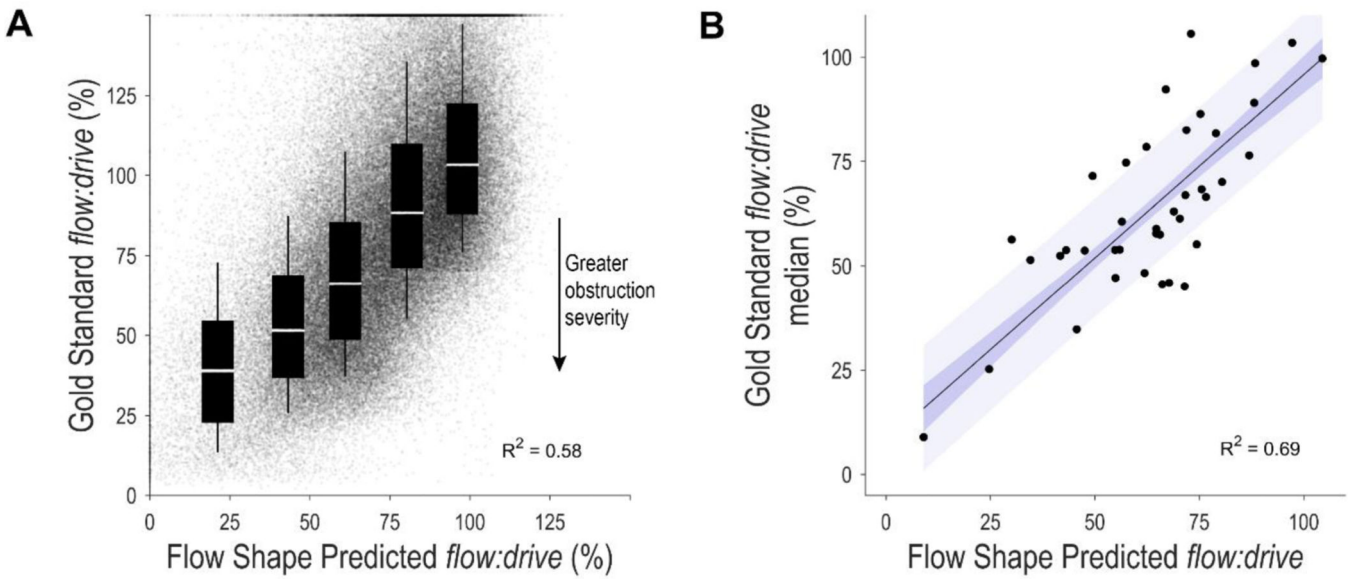

Figure 3:

Airflow obstruction severity estimated from flow shape (pneumotach) predicts the gold standard in individual breaths **(A)** and individual patients **(B)**. **(A)** Gold-standard versus estimated obstruction severity (*flow:drive*) for individual breaths (sleep and wake), note the strong association (R^2=0.58, P<0.00001). The box plot overlay shows summary statistics (median, IQR, 10^{th} to 90^{th} percentiles) for breaths within each severity classification (normal to very severe). **(B)** Gold-standard versus estimated obstruction severity (*flow:drive*) for individual patients (median of sleep only data, 73,737 breaths), note the strong association (R^2=0.69, p<0.00001, adjusted for AHI p<0.00001).

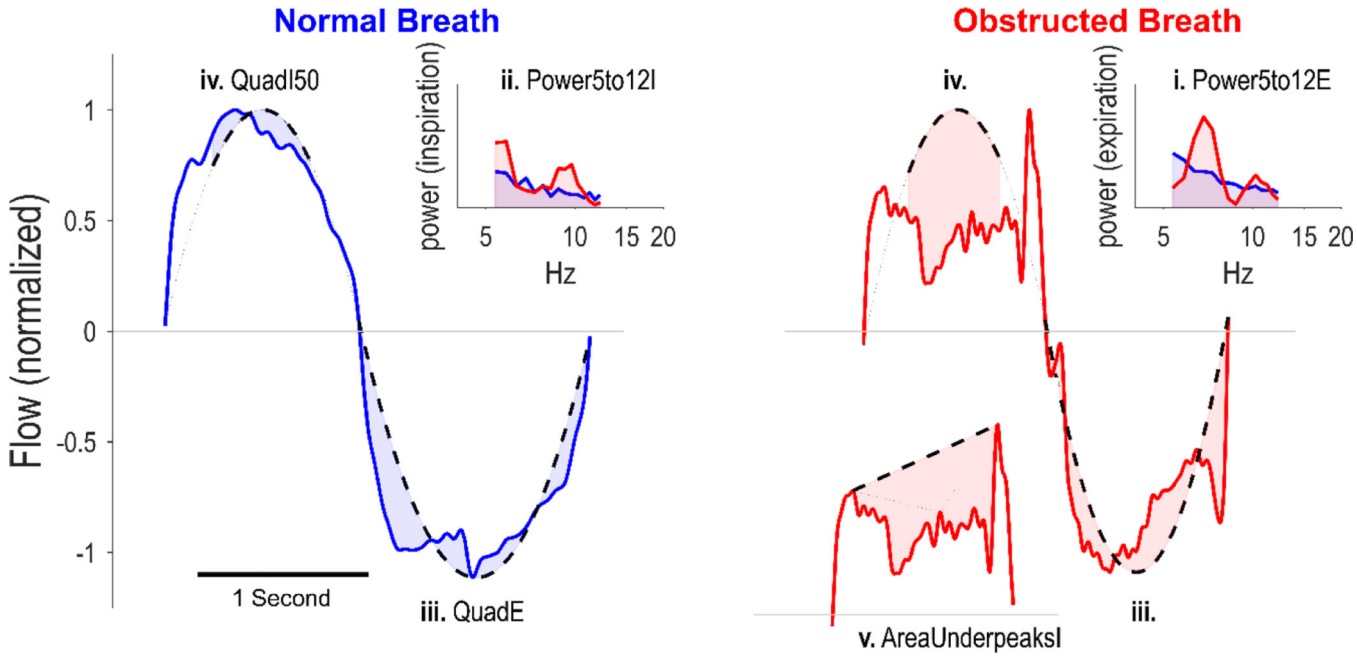

Figure 4:

The five key features in the multivariable airflow obstruction model. An example normal breath (left, blue) and obstructed (right, red) are shown. Increasing values of these features, labelled i-v, indicated greater obstruction. Specifically: **(i and ii)** Power5to12E and Power5to12I quantify the flow variability (power) in 5–12 Hz range for expiration and inspiration respectively; note the area (power) for the obstructed breath (red) is greater than the area for the normal breath (blue). **(iii and iv)** QuadE and QuadI50 quantify the discrepancy between the airflow signal and a matched parabola (same peak amplitude, curved dashed lines), for expiration and inspiration respectively. The absolute difference (area) quantifies the discrepancy (only the middle 50% of inspiration is used, all data for expiration). **(v)** AreaUnderPeaksI captures the degree of *scooping* by quantifying the area under a line joining two inspiratory peaks. A simplified 5-feature model is provided in the Supplement (Table S5, Figures S5 and S6) and performed effectively.

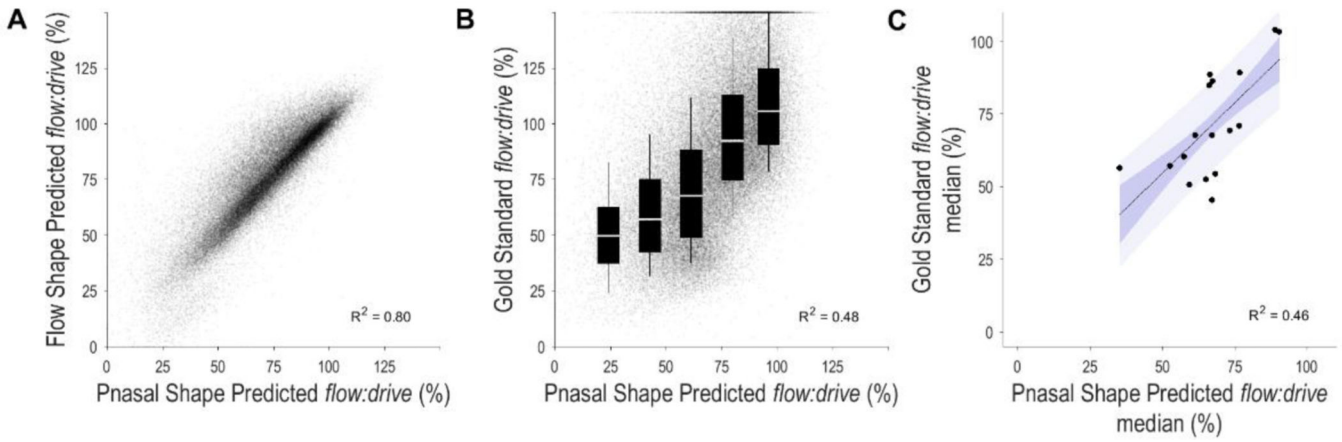

Figure 5:

Nasal pressure analysis of airflow obstruction. **(A)** Scatter plot showing a very strong association (R^2=0.8) between nasal pressure estimated *flow:drive* and pneumotach estimated *flow:drive* values. **(B)** Scatter plot showing a moderate association (R^2=0.48) between nasal pressure estimated *flow:drive* and gold-standard *flow:drive* values for individual breaths. The box plot overlay shows summary statistics (median, IQR, 10th and 90th percentiles) for breaths within each severity classification. A small reduction in performance (compared to pneumotach flow, Figure 3A) appears in the distinction between very-severe and severe obstruction. **(C)** A moderate association is observed between nasal pressure estimated median *flow:drive* and gold-standard patient median *flow:drive* during sleep, including apnoea breaths (R^2=0.46, p<0.003, adjusted for AHI p<0.003). Note that in this subset of patients that include simultaneous oronasal pneumotach flow and nasal pressure signals, there are very few patients with severe and very severe airflow obstruction as shown by gold-standard *flow:drive* <50%. Pnasal, nasal pressure.

Table 1.

Patient characteristics

Characteristic	Comparison to gold standards (N=41)	Nasal pressure vs. pneumotach (N=17)
Demographics		
Age (years)	58±9	59±9
Sex (M:F)	25:16	11:6
Race (Black:White:Asian:Other)	12:28:0:1	3:14:0:0
Body mass index (kg/m^2)	32.4±6.6	31.8±7.5
Neck circumference (cm)	41.3±4.8	41±5.2
Currently treated (CPAP:oral appliance:untreated)	15:2:24	2:1:14
Polysomnography		
OSA severity (normal:mild:moderate:severe)	5:13:7:16	4:8:2:3
Apnoea-hypopnoea index, total (events/hr)	30.5±27.4	15.4±15.7
Apnoea-hypopnoea index, non-REM (events/hr)	30±28	14.5±16.1
Central events, non-REM (% respiratory events)	0.8±3.5	0.5±1.2
Hypopnoeas, non-REM (% respiratory events)	64.4±31.2	80.3±21.7
Arousal Index, non-REM (events/hr)	50.3±24.2	42.7±18.4
Total sleep time (min)	239±92	249±80
Sleep time, spontaneous breathing* (min)	160±96	209±83
Non-REM 1 (% total sleep time)	37±20	37±23
Non-REM 2 (% total sleep time)	48±17	46±18
Non-REM 3 (% total sleep time)	6±7	8±10
REM (% total sleep time)	9±8	9±9

Values are mean±S.D.

*Sleep time available for analysis without physiological tests (part of previous study). OSA severity classes defined as; normal Apnoea-hypopnoea index(AHI)<5, mild 5<AHI<15, moderate 15<AHI<30, and severe AHI>30 events/hr. CPAP = continuous positive airway pressure. OSA = obstructive sleep apnoea. REM = rapid-eye-movement sleep. AHI = apnoea-hypopnoea index. Note the lower AHI in the nasal pressure subset was not by design.

Table 2.

Selection of highest performing unique features in the multivariable airflow obstruction model

Category	Feature Name (in order of importance)	Δ with ↑ obstruction severity	Description/Definition
Fluttering	Power5to12E	Increase	Power in expiratory flow signal [range 5 to 12 Hz]
	Power5to12I	Increase	Power in inspiratory flow signal [range 5 to 12 Hz]
Scooping	QuadE	Increase	Area between expiratory flow shape and a quadratic best fit to 3 points (x,y: start expiration, 0; Te/2, PEF; end expiration, 0)
	QuadI50	Increase	Part area between inspiratory flow shape and a quadratic best fit to 3 points (x,y: start inspiration, 0; Ti/2, PIF; end inspiration, 0). Area taken is from 25th to 75th centiles of inspiratory time.
	AreaUnderPeaksI	Increase	Area between inspiratory airflow signal and connected peaks

Features are in order of importance based on backwards feature elimination (i.e. Power5to12E was the final feature remaining after sequential elimination). The five features listed here are illustrated in Figure 4. A simplified 5-feature model is provided in the Supplement (Table S5, Figures S5 and S6) and performed effectively. Hz, Hertz (cycles/sec). Te, Expiratory time. Ti, Inspiratory time. PEF, Peak expiratory flow. PIF, Peak Inspiratory flow (note PIF was normalised).